# Scanning-probe Raman spectroscopy with single-molecule sensitivity

Catalin C. Neacsu, Jens Dreyer, Nicolas Behr, and Markus B. Raschke
*Max-Born-Institut für Nichtlineare Optik und Kurzzeitspektroskopie, D-12489 Berlin, Germany*
(Received 17 October 2005; revised manuscript received 8 February 2006; published 23 May 2006)

Single-molecule vibrational Raman spectroscopy of malachite green adsorbed on *planar* metal surfaces is achieved by means of optical local-field enhancement provided by a scanning nanoscopic metallic tip. The single-molecule signature is evident from spectral diffusion and a discretization of Raman peak intensities. The optical tip-sample coupling gives rise to a localization of the response down to a sub-10 nm length scale and a Raman enhancement up to $\sim 5 \times 10^9$. This combines vibrational spectroscopy with high resolution scanning-probe microscopy for ultrasensitive *in situ* analysis of individual molecules.

DOI: 10.1103/PhysRevB.73.193406 PACS number(s): 78.67.−n, 33.20.Fb, 33.80.−b, 68.37.Uv

Single-molecule spectroscopy has matured into diverse areas with its most notable contributions in the determination of biomolecular processes even under ambient or physiological conditions.[1–4] So far the detection of individual molecules is largely based on their fluorescence properties, facilitated by the large transition dipole moment. Relying on the molecular electronic transition, this limits the chemical specificity that can be obtained.

In contrast the vibrational Raman signature can provide rich structural information. In this context the discovery of single-molecule sensitivity in surface enhanced Raman scattering (SERS) seemed particularly promising.[5–8] However, with the Raman cross section being of the order $10^{12}$ times smaller compared to fluorescence, SERS relies on the local optical field enhancement at the surface of often poorly defined metallic aggregates or rough surfaces. This, together with the difficulty to select specific target molecules has thus far prevented the application of single molecule SERS as an analytic tool.

The specific plasmonic coupling between closely spaced substrate features is suggested to be largely responsible for the Raman enhancement observed for molecules most likely adsorbed in the nanoscopic gaps between these structural elements.[7] In this study we show that the simple geometry of a sharp metallic scanning probe tip located above malachite green molecules adsorbed on a *planar metal* surface provides sufficient field enhancement to allow for *single molecule* Raman spectroscopy. With the enhancement exceeding corresponding values in previous tip-enhanced Raman experiments[9–11] this allows for probing the Raman response of individual molecules as evident from spectral diffusion and discrete signal intensities.

For our tip-enhanced Raman experiments we apply a confocal epi-illumination and detection geometry. As illustrated schematically in Fig. 1, the tip apex is illuminated side on with 632.8 nm HeNe laser light at an angle of 70° with respect to the tip axis with a maximum fluence of $5-9 \times 10^3$ W/cm$^2$. The polarization of the pump excitation and emitted Raman light can be set independently using polarizing optics. The tip-scattered light is spectrally selected using a notch filter and an imaging spectrograph, and detected with a $N_2$(l)-cooled charged-couple device (CCD) detector. To ensure sufficient sensitivity spectra are acquired with the resolution limited to 25 cm$^{-1}$ (3 meV). The tapered Au metal tips we produce by electrochemical etching as described previously[12] with tip radii down to ~10 nm as characterized by electron microscopy. The tips are mounted to a quartz tuning fork of a shear-force atomic-force microscope (AFM).

Monolayer (ML) and submonolayer coverages of the triarylmethane dye malachite green (MG) were prepared by spin coating from dilute (0.03–0.3 mM) ethanolic solution. Smooth gold surfaces were produced by vacuum evaporation onto cover glass substrates and it was verified by near- and far-field scanning that the gold surfaces itself do not exhibit any SERS effects. With the pump photon energy of 1.96 eV, as indicated in the optical absorption spectrum shown in Fig. 1, this leads to a resonant Raman excitation via the $S_0$-$S_1$ electronic transition of the conjugated $\pi$-electron system.

Figure 2(a) shows the spectrally resolved tip-scattered Raman signal during approach of ~1 ML of MG on gold (2 nm/step, 1 s acquisition time per spectrum). We observe a strongly enhanced and spatially highly localized Raman response for the pump and detected light polarized parallel with respect to the tip axis. The enhancement is confined to a tip-sample spacing of just several nanometers and correlated with the apex radius of the tip. In Fig. 2(b) representative

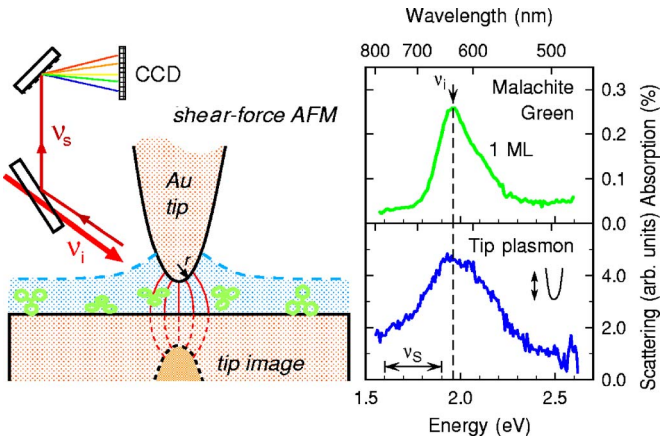


FIG. 1. (Color online) Experiment (left): Tip-scattered and enhanced Raman response of molecules in the tip-sample gap. Right: Absorption spectrum of one surface monolayer of malachite green (top). The plasmon resonance of a representative Au tip (bottom) as evident from the spectral dependence of linear light scattering gives rise to both, strongly enhanced pump ($\nu_i$) and Stokes Raman fields ($\nu_s$) at the tip apex.

 

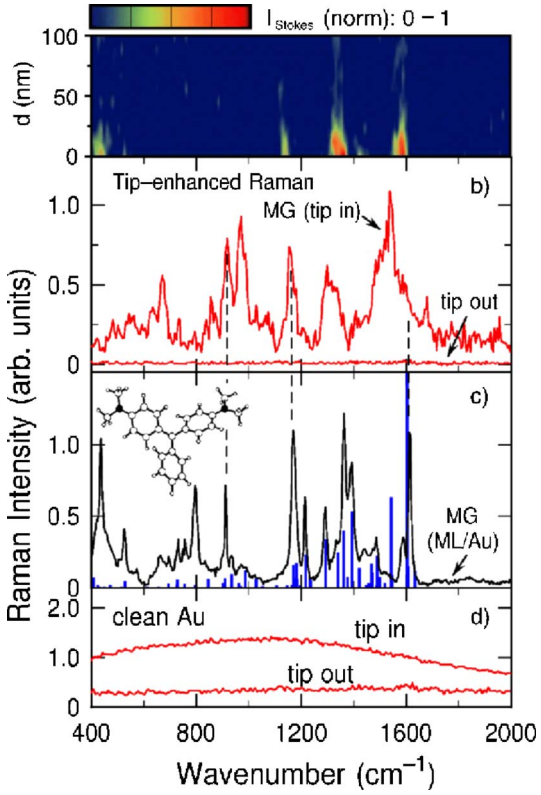


FIG. 2. (Color online) Tip-enhanced vibrational Raman response and corresponding distance dependence (a) of ~1 ML malachite green on a flat Au surface. Comparison of the tip-enhanced Raman response (b) with a corresponding far-field micro-Raman spectrum (c) of the same MG surface layer and the normal mode analysis based on a DFT calculation. The simultaneous near-field enhancement of a fluorescence background largely emerges from the Au-tip apex itself as evident from the control experiment without MG (d).

Raman spectra are shown with the tip in force feedback at $d=0$ nm,[13] versus sample retracted by several 100 nm. The increase in Raman response is accompanied by a weak rise in a spectrally broad fluorescence background which has been subtracted in Figs. 2(a) and 2(b). With the molecular fluorescence being quenched due to the electronic coupling to the metal substrate, this emission can largely be attributed to the enhancement of the intrinsic tip fluorescence[16] as evident from the control experiment shown in Fig. 2(d) for a clean Au surface.

In Fig. 2(c) the far-field Raman spectrum from the same sample is shown for comparison. The spectrum closely resembles that in aqueous solution[17] indicating that the molecules are physisorbed in isotropic orientation at the surface. The tip-enhanced Raman response is notably different in terms of the relative peak amplitudes compared to the far-field Raman spectrum. This characteristic difference is the result of the strong optical field localization, and related to different selection rules for the tip-scattered Raman response, akin to SERS, as discussed below.[18] For weak enhancement the tip-scattered spectra resemble the far-field response more closely. The tip-enhanced Raman spectra are reproducible for a given tip, but their spectral details vary from tip to tip as

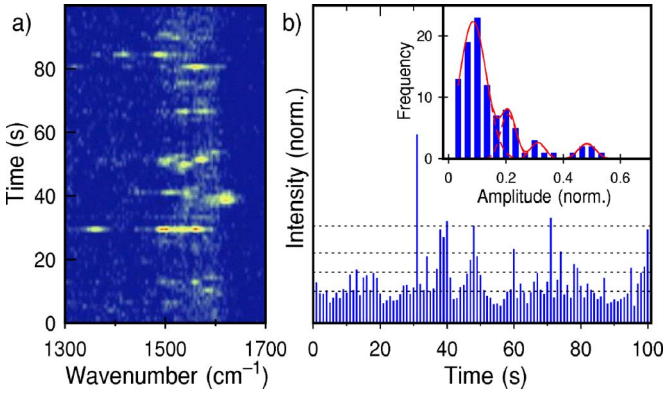


FIG. 3. (Color online) Time series of tip-scattered Raman spectra for a submonolayer MG surface coverage (a). The spectral diffusion observed is characteristic for observing single MG molecules. (b) Temporal variation of the intensities of the integrated 1480–1630 $cm^{-1}$ Raman band with 170–230 counts $mol^{-1}$ $s^{-1}$ (dashed line increment). From the corresponding histogram (inset) a discretization of Raman intensities can be seen.

evident from, e.g., the spectral differences between the data in Figs. 2(a) and 2(b) which were taken with different tips. The decay and subsequent disappearance of the spectral response due to the eventual bleaching on time scales of 100's of seconds depending on enhacement is uniform, i.e., maintaining the relative peak amplitudes. This excludes that molecular decomposition products significantly contribute to the Raman response observed. In addition, transfer or binding of molecules to the tip is unimportant as evident from the absence of any Raman response approaching a clean surface region with a tip which has previously been exposed to a MG covered region.

With the lateral confinement of the tip-enhancement within a ~10 nm diameter surface region and a molecular density of $\sim 1/\mathrm{nm}^2$ we estimate that the signal observed in Fig. 2(b) originates from of order 100 molecules. For the subsequent experiment we resort to a sample prepared with submonolayer surface coverage adjusted to expect on average $<1$ molecule under the tip-confined area of $\sim 100$ $nm^2$. Corresponding tip-scattered Raman spectra measured in a time series with 1 s acquisition time for each spectrum are shown in Fig. 3(a). Here, the tip has been held at constant distance $d \simeq 0$ nm above the sample as established by shear-force feedback with a rms stability of $\lesssim 1$ nm.

The temporal variations of relative peak amplitudes and the fluctuations in spectral position observed are characteristic signatures of probing a single emitter in terms of an individual molecule. Comparing the Raman signal intensity in this experiment with the ensemble measurement verifies the interpretation of the observation of single molecule Raman emission. Figure 3(b) displays the integrated 1430 $cm^{-1}$ to 1650 $cm^{-1}$ spectral intensity for the data in Fig. 3(a) for 100 s before the molecules bleached. The signal intensities cluster with intervals of 170–230 counts $s^{-1}$. This manifests itself in the corresponding histogram in an asymmetric distribution with discrete peaks (inset). This behavior is qualitatively reproducible for experiments with the same surface coverage. It can be interpreted as the Raman emission from

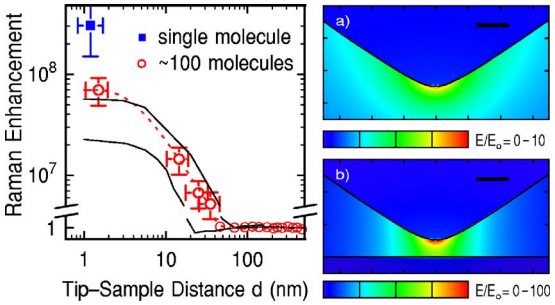


FIG. 4. (Color online) Raman enhancement as a function of tip-sample distance. Representative variations of the total Raman signal for representative tips (solid lines) and the enhancement of just the 1590 $cm^{-1}$ mode (open circles) are shown. Calculated local field distribution and enhancement $E/E_0$ for a Au hyperbolic model tip with $r=10$ nm, free standing (a) vs near Au sample at $d=5$ nm distance (b). Scale bar=10 nm.

$n=0$ (noise peak), 1, 2, and 3 molecules being probed under the tip as suggested by Kneipp *et al.*[5] This assignments is corroborated from experiments with different surface coverages: For lower coverages only the $n=0$ and 1 peaks remain. With increasing coverage the distribution converges to a narrow random Gaussian distribution which is observed for monolayer coverages.

In contrast to SERS where the quantification of the enhancement is a difficult task in general, for the tip-scattering experiment, the enhancement factor can be derived from comparison of tip-enhanced versus far-field response of the same surface monolayer. The resulting distance dependence of the Raman enhancement for the data shown in Fig. 2 and other data for different tips are summarized in Fig. 4.

In our experiment we expect the enhancement to be purely electromagnetic in origin. From the classical description of the macroscopic Raman polarization at the Stokes frequencies $\nu_s$, $P(\nu_s)=N\alpha_{ba}F(\nu_s)F(\nu_i)E(\nu_i)$, where $N$ is the number of molecules, $\alpha_{ba}$ the Raman tensor, and $F(\nu_s)$ and $F(\nu_i)$ the local field factors for the Raman scattered and pump laser field $E(\nu_i)$, respectively, the total Raman enhancement factor $M$ is given by $M=F^2(\nu_i)F^2(\nu_s)$.[19] Assuming $F(\nu_s)$ and $F(\nu_i)$ to be similar given the spectrally broad tip plasmon response, the observed enhancement of $2\times10^7-3\times10^8$ would correspond to average local field factors of 70–130. Considering the Fresnel factor for the planar gold surface this would translate into a Raman enhancement of up to $5\times10^9$ for the tip-enhanced compared to the free molecule response.

From comparison of different tip materials as well as pump and Raman polarizations we find that the source of this strong amplification of the local optical field for the Au tips is the excitation of the axial plasmon resonance of the tip.[12] That plasmon mode is evident from the spectral tip Rayleigh scattering response,[12] as shown in Fig. 1, and it gives rise to a local field enhancement in the range of 10 to 25 for free standing tips.[20] In the presence of the metal surface, strong optical coupling between the metallic tip and substrate is effective. This coupling is a manifestation of the boundary conditions for the optical field in the gap imposed by the substrate plane (mirror image).[21] The effect is seen in Fig. 4 for the field distribution calculated for a hyperbolic tip of apex radius $r=10$ nm with (b) and without (a) sample.[22] The presence of the surface leads to a further increase in the lateral field confinement and to a local field enhancement an order of magnitude larger compared to corresponding values for the bare tip. With values for the local field enhancement of order 10 at the apex of the bare tip and 70 at the substrate surface in the presence of the tip, this model calculation is in good accordance with these and other experimental results[24] and more accurate theoretical descriptions.[24] This tip-sample coupling resembles the situation of recent studies of lithographic surface optical dipole antennas where an analogous pronounced field enhancement with decreasing gap width was demonstrated.[25,26]

To facilitate the identification of the underlying Raman selection rules we performed a computation of the normal modes and polarization derivative tensor elements $\partial\alpha/\partial Q$ for the MG anion using density functional theory [B3LYP/6-31$G(d,p)$] as implemented in Gaussian03.[27] The vibrational Raman frequencies obtained, scaled by a factor of 0.975 are shown in Fig. 2(c). The majority of intense Raman modes can be attributed to modes either localized at the phenyl ring or delocalized over the two dimethylamino phenyl rings.

The pronounced spectral difference between the tip-enhanced and far-field Raman response resembles the observation frequently made in SERS. Aside from orientational effects, these spectral variations are typically interpreted to arise from conformational changes and/or transient covalent binding of the molecule at "active sites." With that being excluded in the tip-enhanced Raman geometry as discussed above, this indicates that purely electromagnetic mechanisms can already induce the kind of spectral selectivity observed.

Different Raman symmetry selection rules can come into play due to the large optical field gradient $\nabla E$ in the tip-sample gap.[18] This would allow, e.g., for the Raman emission from IR active modes ($\propto\alpha_{ba}\nabla E$).[28] The tip-enhanced Raman spectra, however, show no resemblance to the few IR-active modes of MG as measured in KBr and identified with the help of the density functional theory (DFT) calculation. In addition, the field gradient can also couple to vibrations via the derivative of the quadrupole polarizability $A_{ijk}$ of a mode ($\propto\partial A_{ijk}/\partial Q\nabla E$).[18] With $\alpha_{ab}$ and $A_{ijk}$ transforming differently in terms of symmetry and their ratio being highly mode dependant this could account for the mode selectivity observed in tip-enhanced Raman scattering. Although the determination of $A_{ijk}$ is still deemed challenging for large molecules it might contribute to a unified description of the underlying processes, given the well characterized structural environment in tip-enhanced Raman in contrast to most SERS experiments. It might also help to resolve the striking observation that the strength of the calculated four modes at 846, 988, 1029, and 1544 $cm^{-1}$ are overestimated by DFT as compared to the far-field spectra, but are modes found to be strongly enhanced in the tip-enhanced Raman spectra.

Another yet unresolved issue in most surface enhanced experiments is the source of the spectral diffusion and intensity fluctuations observed in connection with high enhancement factors. In our experiments the observations of distinct peaks in the histogram (Fig. 3) can be interpreted by a ran-

dom surface diffusion of MG in and out of the near-field confined surface area under the tip facilitated by the thin, most likely liquid water layer on the gold surface.[14,15] The probability of finding on average $\bar{N}$ molecules under the tip would then follow a Poisson distribution $P(n)=\frac{\bar{N}^n}{n!}e^{-\bar{N}}$ in rough agreement with the experiment. In addition, the possibility for optical trapping and alignment of MG under the tip has also got to be considered. With the local pump intensity of $7\times10^7$ W cm$^{-2}$ estimated inside the tip-sample gap and the anisotropic molecular polarizability calculated as $\alpha_{xx}\simeq150$ Å$^3$, $\alpha_{yy}\simeq63$ Å$^3$, and $\alpha_{zz}\simeq22$ Å$^3$ a trapping potential energy of order $10^{-4}$ eV results[29] with four distinct local minima corresponding to different relative molecular orientations with respect to the tip axis. However, with this energy being much smaller compared to the thermal energy of $kT=2.6\times10^{-2}$ eV, this cannot explain the discretization of Raman peak intensities in the single molecule response.

Given the correlation of vertical and lateral field confinement with tip apex radius (Fig. 4) the great potential of tip-enhanced Raman scattering was demonstrated previously providing ultrahigh lateral resolution down to 10 nm.[10] However, the sensitivity has often been limited either due to the illumination geometry applied or the use of dielectric substrates. With the enhanced sensitivity demonstrated here using metallic substrates, this experiment parallels the vibrational imaging of single molecules in inelastic electron tunneling at low temperatures.[30] Given the additional virtues of being an optical technique and applicable under ambient conditions this opens new possibilities for vibrational nanospectroscopy of individual chemical and biological structures.

The authors would like to acknowledge insightful discussions with Tamar Seideman and Hans-Hermann Ritze.

[1] H. P. Lu, L. X. Xun, and X. S. Xie, Science **282**, 1877 (1998).
[2] W. E. Moerner and M. Orrit, Science **283**, 1670 (1999).
[3] C. Bustamante, Z. Bryant, and S. B. Smith, Nature (London) **421**, 423 (2003).
[4] S. Weiss, Nat. Struct. Biol. **7**, 724 (2000).
[5] K. Kneipp, Y. Wang, H. Kneipp, L. T. Perelman, I. Itzkan, R. R. Dasari, and M. S. Feld, Phys. Rev. Lett. **78**, 1667 (1997).
[6] S. Nie and S. R. Emory, Science **275**, 1102 (1997).
[7] H. Xu, E. J. Bjerneld, M. Käll, and L. Börjesson, Phys. Rev. Lett. **83**, 4357 (1999).
[8] A. M. Michaels, M. Nirmal, and L. E. Brus, J. Am. Chem. Soc. **121**, 9932 (1999).
[9] R. M. Stöckle, Y. D. Suh, V. Deckert, and R. Zenobi, Chem. Phys. Lett. **318**, 131 (2000).
[10] A. Hartschuh, E. J. Sánchez, X. S. Xie, and L. Novotny, Phys. Rev. Lett. **90**, 095503 (2003).
[11] B. Pettinger, B. Ren, G. Picardi, R. Schuster, and G. Ertl, Phys. Rev. Lett. **92**, 096101 (2004).
[12] C. C. Neacsu, G. A. Steudle, and M. B. Raschke, Appl. Phys. B **80**, 295 (2005).
[13] The tip-sample distance $d\approx0$ nm is defined by a 30–40 % decrease in the tuning-fork shear-force signal. With the corresponding signal trace, characterized by a width of 12 to 14 nm (5 to 95 % damping), the physical tip-sample contact is expected at $d\sim-5$ to $-6$ nm (Ref. 14). The damping is mostly due to viscous forces exerted by a water layer of several nm thickness formed at the surface (Ref. 15) under ambient conditions.
[14] K. Karrai and I. Tiemann, Phys. Rev. B **62**, 13174 (2000).
[15] R. Brunner, O. Marti, and O. Hollricher, J. Appl. Phys. **86**, 7100 (1999).
[16] M. R. Beversluis, A. Bouhelier, and L. Novotny, Phys. Rev. B **68**, 115433 (2003).
[17] H. B. Lueck, D. C. Daniel, and J. L. McHale, J. Raman Spectrosc. **24**, 363 (1993).
[18] J. A. Creighton, *Spectroscopy of Surfaces* (Wiley, Chichester, 1988), Chap. 2, p. 37.
[19] M. Moskovits, Rev. Mod. Phys. **57**, 783 (1985).
[20] C. C. Neacsu, G. A. Reider, and M. B. Raschke, Phys. Rev. B **71**, 201402(R) (2005).
[21] P. Johansson, H. Xu, and M. Käll, Phys. Rev. B **72**, 035427 (2005).
[22] Treating the tip as a hyperboloid the local field distribution can be derived analytically in the quasistatic approximation (Ref. 23). From comparison with the computation of the exact Maxwell solution it can be shown that for structural dimensions $\leq\lambda/20$ this method provides a good approximation (Ref. 24).
[23] W. Denk and D. W. Pohl, J. Vac. Sci. Technol. B **9**, 510 (1991).
[24] R. M. Roth, N. C. Panoiu, M. M. Adams, R. M. Osgood, C. C. Neacsu, and M. B. Raschke, Opt. Express **14**, 2921 (2006).
[25] P. Mühlschlegel, H.-J. Eisler, O. J. F. Martin, B. Hecht, and D. W. Pohl, Science **308**, 1607 (2005).
[26] P. J. Schuck, D. P. Fromm, A. Sundaramurthy, G. S. Kino, and W. E. Moerner, Phys. Rev. Lett. **94**, 017402 (2005).
[27] M. J. Frisch *et al.*, Gaussian 03, Revision C.02 (Gaussian, Inc., Wallingford, CT, 2004).
[28] E. J. Ayars, H. D. Hallen, and C. L. Jahncke, Phys. Rev. Lett. **85**, 4180 (2000).
[29] B. Friedrich and D. Herschbach, Phys. Rev. Lett. **74**, 4623 (1995).
[30] B. C. Stipe, M. A. Rezaei, and W. Ho, Science **280**, 1732 (1998); X. H. Qiu, G. V. Nazin, and W. Ho, *ibid.* **299**, 542 (2003).